Discrete Dipole Approximation simulations of gold nanorod optical properties: choice of input parameters and comparison with experiment

Constantin Ungureanu,* Raja Gopal Rayavarapu, and Srirang Manohar†
Biophysical Engineering Group, Institute for Biomedical Technology (BMTI), Faculty of Science and Technology, University of Twente, PB 217, 7500AE, Enschede, The Netherlands

Ton G. van Leeuwen
Laser Center, Academic Medical Center, University of Amsterdam, PB 22700, 1100DE, Amsterdam, The Netherlands and Biophysical Engineering Group, Institute for Biomedical Technology (BMTI), Faculty of Science and Technology, University of Twente, PB 217, 7500AE, Enschede, The Netherlands

(Dated: June 16, 2008)

Gold nanorods have interesting optical properties due to surface plasmon resonance effects. A variety of biomedical applications of these particles have been envisaged and feasibilities demonstrated in imaging, sensing and therapy based on the interactions of light with these particles. In order to correctly interpret experimental data, and tailor the nanorods and their environments for optimal use in these applications, simulations of the optical properties of the particles under various conditions are essential. Of the various numerical methods available, the Discrete Dipole Approximation (DDA) approach implemented in the publicly available DDSCAT code, is a powerful method that has proved popular for studying gold nanorods. However, there is as yet no universal agreement on the choice of the number of dipoles for the discretization, on the shape used to represent the nanorods and on the dielectric function of gold required for the simulations. We systematically study the influence of these parameters on simulated results. We find large variations in the position of plasmon resonance peaks, their amplitudes and shapes of the spectra depending on the choice of the parameters. We discuss these in the light of experimental optical extinction spectra of gold nanorods synthesized in our laboratory. While making some recommendations to improve accuracy of the simulation results, we show that much care should be taken and prudence applied before DDA results be used to interpret experimental data and to help characterize nanoparticles synthesized.

PACS numbers:

I. INTRODUCTION

Gold nanoparticles exhibit striking optical properties due to the phenomenon of surface plasmon resonance.[1] Conduction electrons are set into resonant oscillation at certain wavelengths of incident light, which is manifested in a peaking in the interactions between photons and the nanoparticles. In general, the wavelengths at which the plasmon peaks occur are dependent not only on size and shape but also coupling between particles and properties of the embedding medium. In the case of spherical gold nanoparticles with diameters < 20 nm dispersed in water, the scattering and absorption spectra show sharp and narrow peaks at around 520 nm. Due to their asymetry, gold nanorods (GNRs) show two plasmon resonances: a longitudinal mode and a transverse mode, due to electron oscillations along the major and minor axes of the particles respectively. The transverse plasmon peak remains in the vicinity of 520 nm, but the longitudinal plasmon (LP) resonance peak can be tuned to occur in the visible and the near-infrared (NIR) wavelengths by changing, for example the aspect ratio of the particles. In addition to maxima in the scattering and absorption, photoluminescnce effects have also been observed. Further, certain Raman emitting molecules adsorbed on such particles exhibit surface-enhanced Raman scattering (SERS) due to the coupling of the molecules' electronic states with the plasmon resonance band.

Biomedical applications of GNRs based on these properties are emerging rapidly and include sensing, imaging and therapy. The light scattering and emission properties of GNRs have promoted their use as excellent labels in studying biological and biochemical processes in cells using dark-field microscopy,[2,3,4] Raman spectroscopy,[5,6] optical coherence tomography,[7,8] and multiphoton microscopy.[9,10] Further, based on the wavelength dependence of the plasmon resonance on the refractive index of the local environment, GNRs have been shown to perform as biochemical sensors.[11] Absorption of light by GNRs is followed by predominantly nonradiative de-excitation processes and the released heat and subsequent temperature rise has applications in improving photoacoustic signals.[12,13] Further the temperature rise can be made sufficiently high to cause cell-death by hyperthermia which has potential for important therapeutic applications.[14,15,16] In the last one mentioned applications, the ability to red-shift LP peaks by tailoring

*Electronic address: C.Ungureanu@utwente.nl
†Electronic address: S.Manohar@utwente.nl

the dimensions of the GNRs coupled with the fact that biological tissue is relatively transparent in the red and NIR wavelengths makes GNRs very attractive.

Modelling the optical properties of GNRs and their dependence on various particle and environmental conditions is of paramount importance in deciding applications and/or tailoring conditions to exploit performance optimally in these applications. Further, comparison of experimental data with simulated optical properties is a means of characterizing samples of nanoparticles in terms of the various parameters such as size, geometry, concentration, dispersity that these properties are known to depend on. Modelling efforts in the recent past have concentrated on the Discrete Dipole Approximation (DDA) method,[17] the most popular realization of which is the DDSCAT code.[18]

Since the early studies by the group of Schatz and van Duyne[19] where the applicability of the DDA approach to simulate the extinction spectra of small metallic particles was shown, a variety of shapes and compositions have been studied including gold nanorods.[20,21,22,23] Lee and El-Sayed[24] used DDSCAT to show the relative contributions of scattering and absorption to the extinction as a function of aspect ratio and medium refractive index, as well as a preliminary study of the effect of end-cap shape. Further studies from the El-Sayed group looked at the effect of effective particle size and composition.[25,26] Prescott and Mulvaney[27] further investigated effects of different capping geometries to the basic cylinder shape. They also showed the importance of using polydispersity in simulating extinction spectra. Kooij and Poelsema[28] studied various morphologies to represent nanorods and showed the influence of electron surface scattering due to particle finite size effects.

While the knowledgebase is considerable in DDA applications for gold nanorods, there are inconsistencies in the choice of various parameters required for the simulations. In this article we call attention to this problem by showing the profound influence that these parameters have on the results. The number of dipoles used to approximate the continuum macroscopic particle is shown to change the results even if general accuracy guidelines are maintained. The effect of morphology - whether ellipsoid, rectangular, cylindrical or hemispherically capped-cylinder has been studied in the past, with observations that the one or other gives a good agreement to experiment.[21,27,28] We show that this must be regarded with circumspection since in combination with a different source of the dielectric function of gold, fortuitous agreements may be found in certain cases. All in all, we show that there are several issues that should be considered before DDA results can be used to correctly interpret experimental data and to help characterize nanoparticles synthesized.

II. MATERIALS AND METHODS

A. Gold nanospheres and nanorods

Gold spheres of 25 nm were purchased from Aurion BV (Wageningen, The Netherlands) and spheres of 60 nm from British Biocell International (UK). GNRs were synthesized in the laboratory using the seed-mediated growth method of Nikoobakht and El-Sayed.[29,30] In this wet-chemistry method, preformed gold spheres form the seed on which metal is grown along preferential directions directed by the surfactant cetyltrimethylammonium bromide (CTAB) in the presence of silver nitrate ($AgNO_3$). Excellent tuning of aspect ratios is achieved by changing the volumes of $AgNO_3$ in the growth solution. Details may be found in Ref. 30 but we summarize the protocol here. Gold spheres as seed were prepared by reducing 5 ml 0.0005 M tetrachloroauric acid with 0.6 ml 0.01 M sodium borohydride in the presence of 5 ml 0.2 M CTAB. Within 15 minutes, 0.014 ml of this seed solution was added to growth solutions containing 5 ml 0.0005 M tetrachloroauric acid, 5 ml 0.2 M CTAB, 0.07 ml 0.1M ascorbic acid and [0.05, 0.1, 0.25] ml of 0.006 M $AgNO_3$.

Sizes and shapes of the nanoparticles were examined in high resolution Scanning Electron Microcopy (HR-SEM) digital images; dimensions measured from at least 250 particles using the NI-Vision module (Labview, National Instruments). Extinction spectra of the nanoparticles were measured using the Shimadzu PC3101 UV-Vis -NIR spectrophotometer.

B. The DDSCAT package

DDSCAT 6.1[18] is a FORTRAN package that implements the DDA method to simulate interaction of electromagnetic radiation with particles of arbitrary shape and composition. The method is described in detail elsewhere.[31,20,21,22,23] Briefly, the particle is subdivided into N polarizable points, located on a cubic lattice with an interdipole distance d given by $V = Nd^3$ where V is the volume of the particle.[18] The radiation scattered and absorbed by the target is computed taking into consideration dipole-dipole interactions. A large variety of particle shapes may be studied where the size of the particle is represented by the effective radius $r_{eff} = (3V/4\pi)^{1/3}$, which is the radius of a sphere having a volume equal to that of the particle. The output parameters from the simulation are extinction, absorption and scattering efficiencies (Q_{ext}, Q_{abs}, Q_{sca}) which yield the corresponding cross-sections of the particle when multiplied by πr_{eff}^2. In all simulations, the results are the average of the two cases of incident light polarization perpendicular to nanorod transverse and longitudinal axes respectively. All DDSCAT simulations were run on the Netherlands National Computer cluster (LISA).

C. Choice of number of dipoles in DDSCAT

For accuracy, Draine and Flatau[18] recommend that the number of dipoles N used to discretize the particle, is chosen to satisfy criterion:

$$|m|kd < 0.5, \tag{1}$$

where m is the complex refractive index of the target material, $k = 2\pi/\lambda$ is the angular wavenumber with λ the wavelength of light and d the inter-dipole distance. While still maintaining this accuracy criterion, we studied the effect of the number of dipoles on the simulation results. Extinction spectra of nanorods with typical dimensions were simulated using a variable number of dipoles between 4500 to 53000. For this study the nanorods were represented as hemispherically-capped cylinders (see next subsection II D), the dielectric function of gold was chosen from Johnson and Christy[32] (see subsection II E) and the refractive index of the environment was chosen as that of water (1.33).

D. Choice of nanorod shape in DDSCAT

There have been prior studies to investigate the influence of morphology chosen to represent the nanorod shape on simulation results. Lee and El-Sayed[24] and Prescott and Mulvaney[27] showed that varying the end-cap shape from flat to hemispherical red-shifts the wavelength of LP peak. While we use the hemispherically-capped cylinder as approximating the nanorods we synthesize, we extend the work of Kooij and Poelsema[28] and compare simulations of ellipsoidal, cylindrical, rectangular and hemispherically-capped cylinder shape with experimental spectra. Henceforth, as in Ref.24 we refer to the last shape as nanorod shape.

E. Choice of dielectric function of the material in DDSCAT

Information regarding the target composition is introduced via the complex dielectric function $\epsilon_m = \epsilon_1 + i\,\epsilon_2$ or $m = n + ik$. Prior reports have used without justification experimental data tabulated by either Johnson and Christy,[32] Palik[33] or Weaver.[34] Further, sometimes bulk values and at other times size corrections modifications to account for surface damping have been used. References 20,22,23,26,35 extracted the bulk values from Johnson and Christy[32]; references 21,24,25,28 used bulk values from Palik[33]; reference 27 used the size-corrected values from Weaver.[34] In this work we compare results using dielectric functions from all the 3 sources both bulk and surface-corrected. Irregularities in the data of Palik[33] were removed to obtain a smooth variation of dielectric function in the values.[28] Size correction was performed according to the standard manner[20] by including an additional damping term to account for the collision of conduction electrons with the particle surface. This is expressed as:

$$\epsilon_m = \epsilon_b + \Delta\epsilon \text{ where,} \tag{2}$$

$$\Delta\epsilon = \frac{\omega_p^2}{\omega(\omega + i/\tau)} - \frac{\omega_p^2}{\omega(\omega + i/\tau + i/\tau_a)} \tag{3}$$

where ϵ_b is the experimental bulk metal value of the dielectric function, ω_p is the plasma angular frequency, $1/\tau$ is the damping constant and $1/\tau_a$ is the surface damping term given by ν_f/r_{eff} with ν_f the Fermi velocity. For size correction, an effective radius of 12 nm was used which is the average effective radius for gold nanorods synthesized in our laboratory.

TABLE I: Mean values of size-related parameters for gold nanorod samples.

Batch	LP peak position (nm)	length (nm)	width (nm)	aspect ratio
I	675	44.8±4.1	19.8±2.9	2.26±0.3
II	765	45.1±5.5	15.8±3.1	2.85±0.6
II	850	51.0±4.4	14.1±2.1	3.62±0.6

III. EXPERIMENTAL AND NUMERICAL RESULTS

A. Gold nanorod synthesis

The synthesis protocol yielded GNRs with longitudinal plasmon (LP) resonant peaks designed to occupy wavelengths in the region 675 -850 nm by increasing the $AgNO_3$ volume in the growth solution.[30] Absorbance spectra of three sets of GNRs with aspect ratios 2.26, 2.85 and 3.62 are shown in Fig. 1(a). The positions of the LP peaks due to conduction electron oscillations along the long-axes of the particles are seen to red-shift with increasing aspect ratios. The transverse plasmon peaks due to oscillations along the short-axes remain steady in the region of 516 nm. Figure. 1(b) is a HR-SEM image of a typical selection of GNRs with aspect ratio 2.85. Information regarding mean values of length, width, aspect ratio and position of the LP peak are presented in Table.1.

B. Number of dipoles

In the case of gold nanospheres no large variations in the simulation results were observed for varying dipole numbers above the accuracy criterion (Eq. 1) which was also reported by Félidj *et al*[20]. This is due to the symmetry of the sphere and the absence of vertices or end-faces where the interdipole spacing becomes crucial.

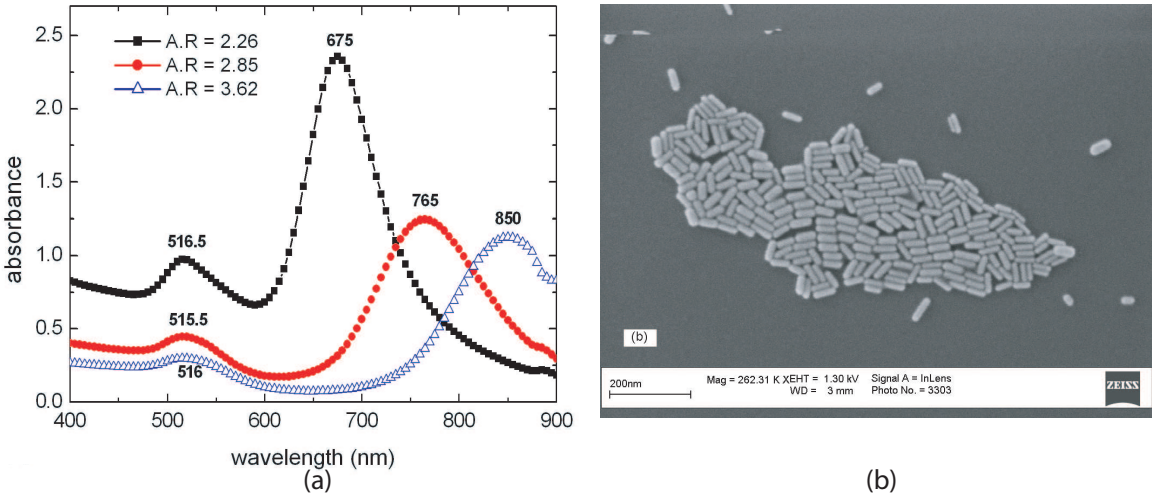

FIG. 1: Absorbance spectra of gold nanorods with aspect ratios 2.26, 2.85 and 3.62. (b) High-resolution Scanning Electron Microscope (HR-SEM) image of particles with aspect ratio of 2.85.

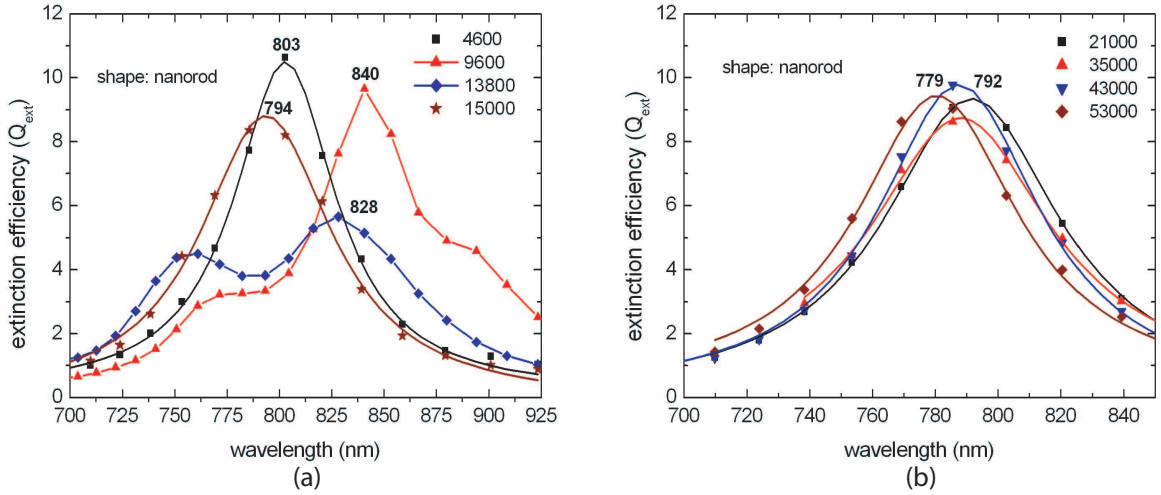

FIG. 2: Calculated extinction spectra in the region of the LP peak of gold nanorods with aspect ratio of 2.85 for varying numbers of (a) 4600-15000 and (b) 20000-53000 dipoles.

Figure. 2(a) shows the simulated extinction spectrum in the region of the LP peak using numbers of dipoles from 4,600 to 15,000; fig. 2(b) with dipole numbers ranging from 21,000 to 53,000. These simulations used nanorod shaped particles, with aspect ratio 2.85 and dielectric function from Johnson and Christy.[32] It is seen that there are inadmissibly large changes in amplitudes and wavelengths of extinction efficiency at lower numbers of dipoles even to the extent of double peaks occurring. It should be noted that in all cases the accuracy criterion (Eq. 1) has been obeyed. Above approximately 15,000 dipoles there is convergence into single peaks which are stable in both wavelength and amplitudes to within 0.1% and 9% respectively with further increasing dipole numbers. The position of the LP for simulations with dipoles 15,000 and above is 789±8.3 nm, which is however different from the experimentally derived peak which at 764 nm (Fig. 1(a)).

Computational time in DDSCAT is proportional to the cube of the number of dipoles N^3, and also scales with the wavelength resolution and range. We found that for reliable results dipole numbers above 30,000 were required; above this, computing times were inordinately high for marginal gains in reliability.

C. Shape

Figures. 3(a), 3(b) and 3(c) show the simulated extinction spectra for GNRs with aspect ratios 2.26, 2.85 and 3.62 when the particle morphology is treated as ellip-

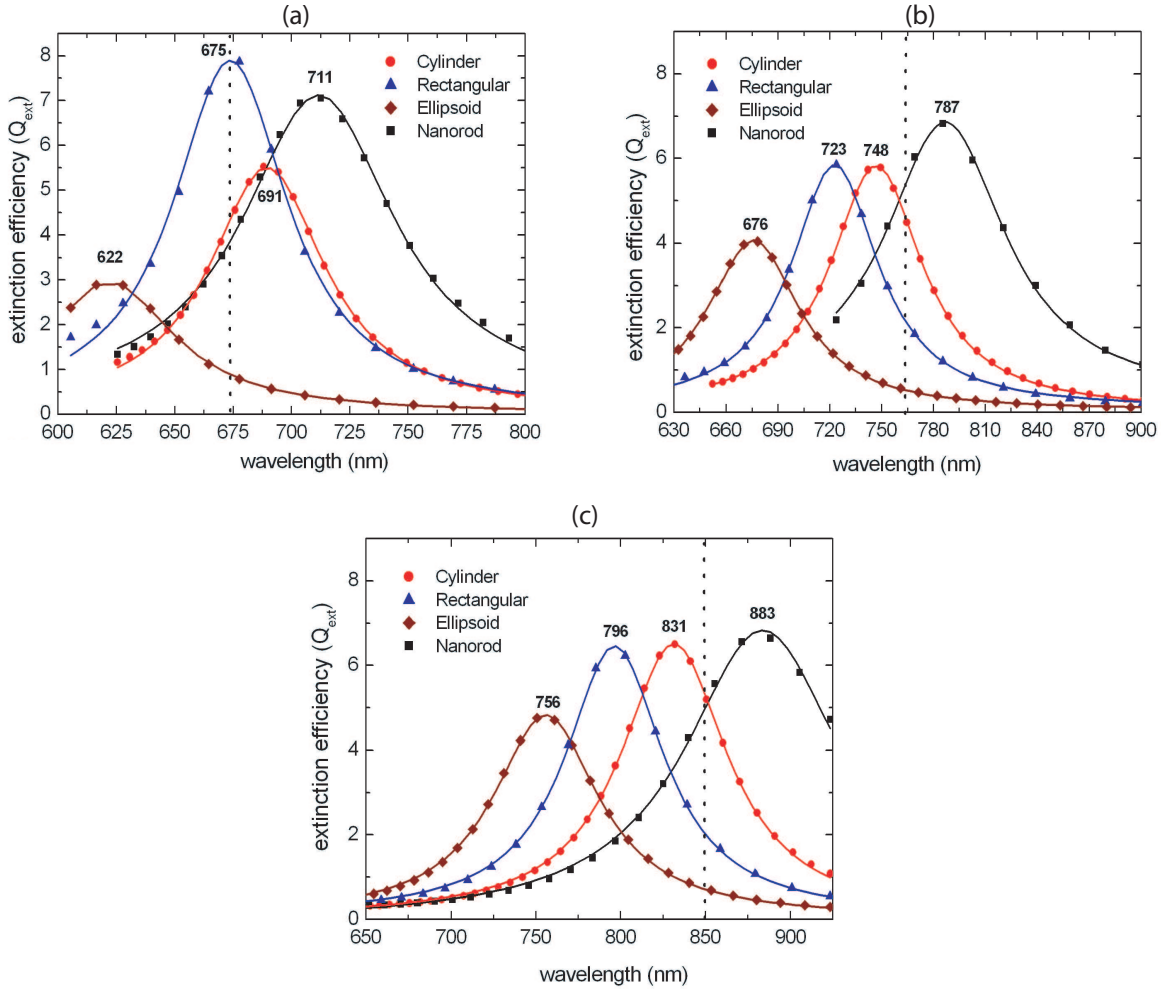

FIG. 3: Calculated extinction spectra in the region of the LP wavelength for a gold nanorod represented by different shapes for aspect ratio (a) 2.26, (b) 2.85 and (c) 3.62. The dotted line marks the experimental derived peak.

soidal, rectangular, cylindrical and nanorod shaped. The positions of the LP maximum from spectrophotometric data of the respective sols are also shown in the graphs with dotted lines. Dipole numbers of 40,000, a refractive index of 1.33 for the environment, and the size-corrected dielectric function from Johnson and Christy[32] were used in the simulations.

There is considerable variation in position, amplitude and width of the resonance maxima with the different shapes as observed earlier.[24,27,28] However, contrary to Ref. 27 and Ref. 36, our simulations with cylinders yield blue-shifted LP peaks when compared with nanorods.

We observe that the experimental maximum position lies between those obtained simulating the cylinder and nanorod shapes in the case of particles with aspect ratios 2.85 and 3.62. In these cases, ellipsoidal and rectangular forms yield positions farthest away from the experimental position of the LP peaks. For an aspect ratio of 2.26, the rectangular form gives a LP position matching experiment.

D. Dielectric function

The real and imaginary parts (ϵ_1 and ϵ_2) dielectric functions (see Eq. 2) extracted from Johnson and Christy,[32] Palik[33] and Weaver[34] are shown in Fig. 4(a) and (b), respectively. In the range 500-600 nm ϵ_1 values from the three sources are closely similar. Values of ϵ_2 from Johnson and Christy[32] and Palik[33] have an offset from each other in this range.

In the near-infrared regions, the data curves of ϵ_1 from the three sources diverge. For ϵ_2, the values from Johnson and Christy[32] and Palik[33] maintain a similar trend with a small constant offset between each other; the ϵ_2 from Weaver[34] is lower and continuously diverges from the other data curves.

The normalized extinction efficiency spectra for gold spheres with diameters 25 nm and 60 nm using bulk and size-corrected (see Eq. 2 and 3) dielectric function values

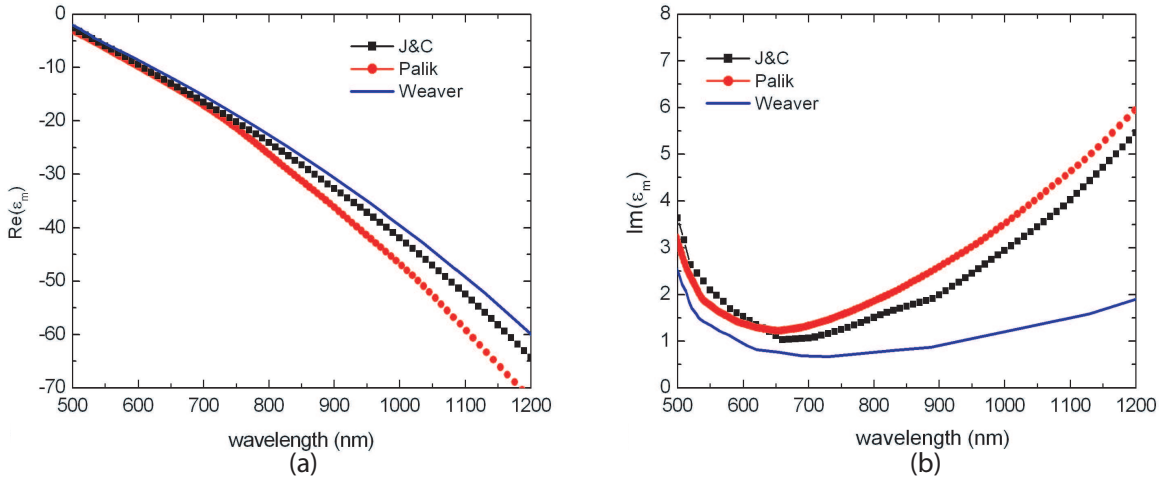

FIG. 4: Bulk dielectric function of gold from Ref. 32, Ref. 33 and Ref. 34.

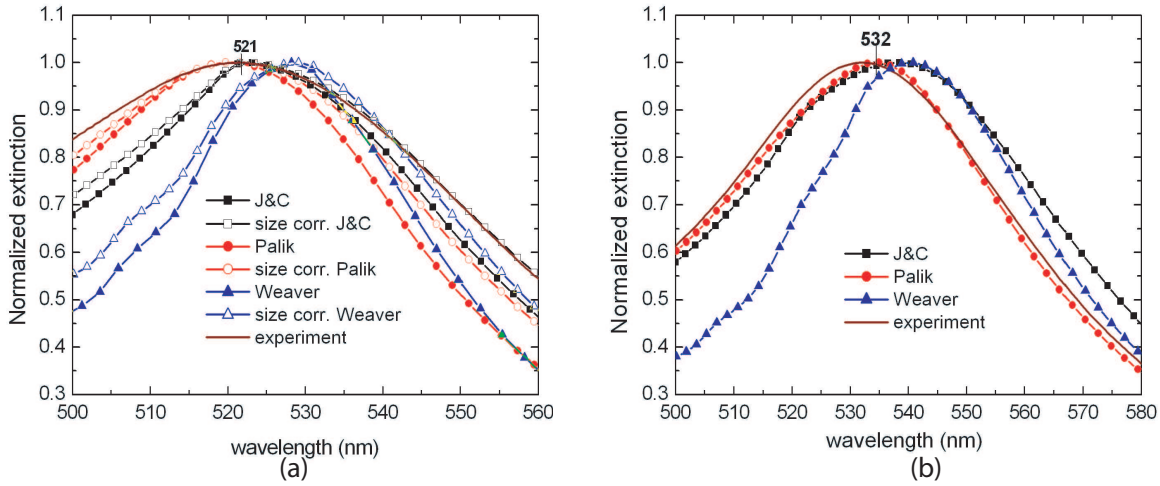

FIG. 5: Comparison of simulated and experimental extinction spectrum of gold sphere: (a) 25 nm diameter and (b) 60 nm diameter.

from the three sources are shown in Fig. 5(a) and (b) respectively. The experimental extinction spectra of the respective sols are also plotted in the figures. Simulations were performed for 40,000 dipoles and a local refractive index of 1.33.

The most significant feature is that the position of the plasmon peak is predicted well within 1% in all cases with a good match to experiment with the exception when data from Weaver[34] was used. This can be explained by the marginal difference between the data from Johnson and Christy[32] and Palik[33] in the region of the spectrum where the sphere's plasmon peak occurs. As expected the size-corrected results while maintaining the resonance maximum position show broadening in the case of the smaller sphere but have hardly any difference for the larger sphere. In the case of the 60 nm sphere the best fit to experiment is obtained with the Palik[33] values; however, no conclusion can be made for the 25 nm sphere.

The simulated extinction spectra using bulk and size-corrected values of dielectric functions for gold nanorods with aspect ratios 2.26, 2.85 and 3.62 are shown in Fig. 6(a), (b) and Fig. 7(a) respectively. The nanorod shape was simulated for 40,000 dipoles and a local refractive index of 1.33. It is clear that there is a wide variation in results obtained with the different sources for the dielectric function. For particles with aspect ratio of 2.85 and 3.62, bulk and size-corrected values from Palik[33] give the resonance maxima close to the experimental values. In all cases the results using data from Weaver[34] are the farthest from experimental values. As expected the size-corrected counterparts of the bulk values do not affect the position of LP peaks but cause a lowering and broadening of the maxima. Amplitude differences between

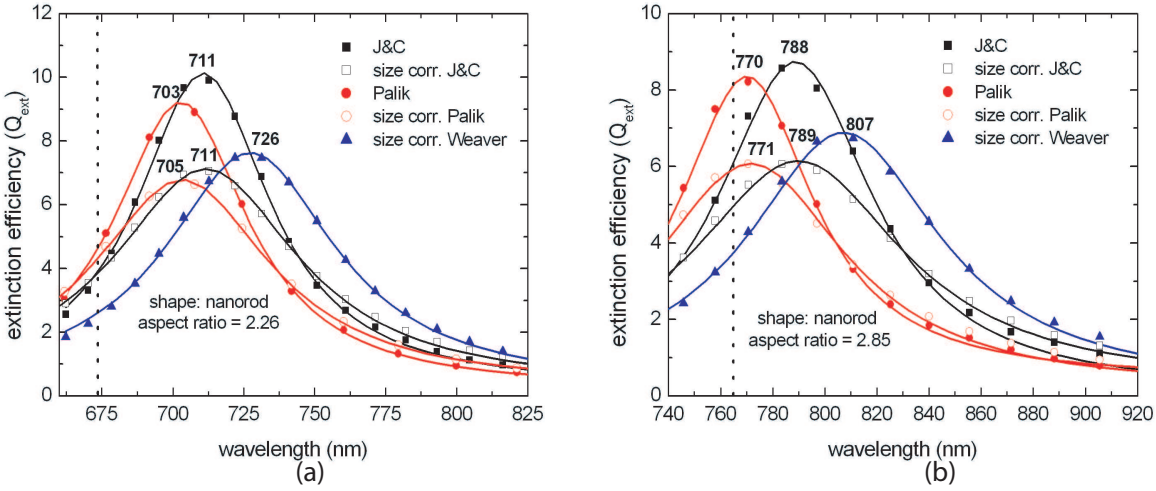

FIG. 6: Simulated extinction spectrum using five different dielectric functions for nanorods with aspect ratios: (a) 2.26 and (b) 2.85.

simulations can be as high as 30% depending on which data sources are considered. Within results from size-corrected or bulk dielectric functions, amplitude variations as high as 10% in amplitude are observed.

The observation of Prescott and Mulvaney[27] that a good match between simulations using data from Weaver[34] with experiment was found when particles were simulated as cylinders was intriguing and we decided to test the same with our experimental data. We too found an excellent match in positions of the resonant maxima between simulations and experiment for samples with aspect ratio 2.85 and 3.62 as shown in Fig. 7(b).

IV. DISCUSSION

The discretization of the continuum target into polarizable points dictates that accuracy depends upon the number of dipoles chosen. Based on numerical studies invoking size and refractive index considerations Draine and Flatau[18] recommended an accuracy criterion (Eq. 1). Based on comparing the resulting granularity from discretization with surface area, wavelength and skin-depth, it was recommended by Félidj *et al*[20] that in order to obtain results accurate to a few percent the inter-dipole distance d should obey $d \leq 8$ nm. We discover for the case of GNRs that even when these general accuracy guidelines are maintained there are variations in band shapes, band positions and peak amplitudes. This is due to the asymmetry of the particles and the presence of tips or end-faces where the interdipole spacing will determine the form of the tip truncation. Between 9000 and 15000 dipoles for the specific case studied (Fig. 2) corresponding to interdipole spacings between 0.93 nm and 0.75 nm we see large discrepancies in the results with the presence of double peaks. Between 15000 and 50000 dipoles corresponding to interdipole spacings 0.75 nm and 0.51 nm there is convergence to the signature LP single peak. The variations in amplitude (Fig. 2) and peak positions however are greater than 5%.

The inaccuracies in the amplitude and position of the LP band for simulations involving numbers of dipoles greater than 15000 are acceptable for applications involving ensemble populations of GNRs such as in photoacoustic imaging and photothermal therapy.[2,12,13,15,16] However, predictions or interpretation of experimental results using these simulations will be unreliable for single-particle or low-number particle studies involving crucial wavelength- and/or amplitude-monitoring.

We confirm previous reports[24,27,28] showing the strong dependence of shape on simulation results. Examination of HR-SEM images of the GNRs synthesized by us, leads us to consider the hemispherically-capped cylinder or nanorod shape as the most serious contender for appropriate morphology of the particles. Cylinders, rectangles and ellipsoids which were also studied have a decreasing order of suitability. Comparison of experimental data with the simulations (Fig. 3) throws up a striking feature, the experimental resonance maximum in 2 cases is pegged in between the peaks from simulations using shapes of cylinder and hemispherically-capped cylinder. This provokes an obvious question: are the end-caps of our GNRs best described by a eccentricity between $e = 0$ for hemispherically-capped and $e = 1$ for cylinder? The influence of eccentricity of the end-cap on simulation results has been systematically investigated by Prescott and Mulvaney.[27] Surprisingly, they observed that in their case, the best fit to experiment was with a pure cylinder shape. These contradictory results may be reconciled by qualifying our simulations and those of Prescott and Mulvaney[27] with the fact that dielectric functions from different sources were used.

The choice of dielectric function is of great importance in the simulations. Figures. 6 and 7 demonstrate this in

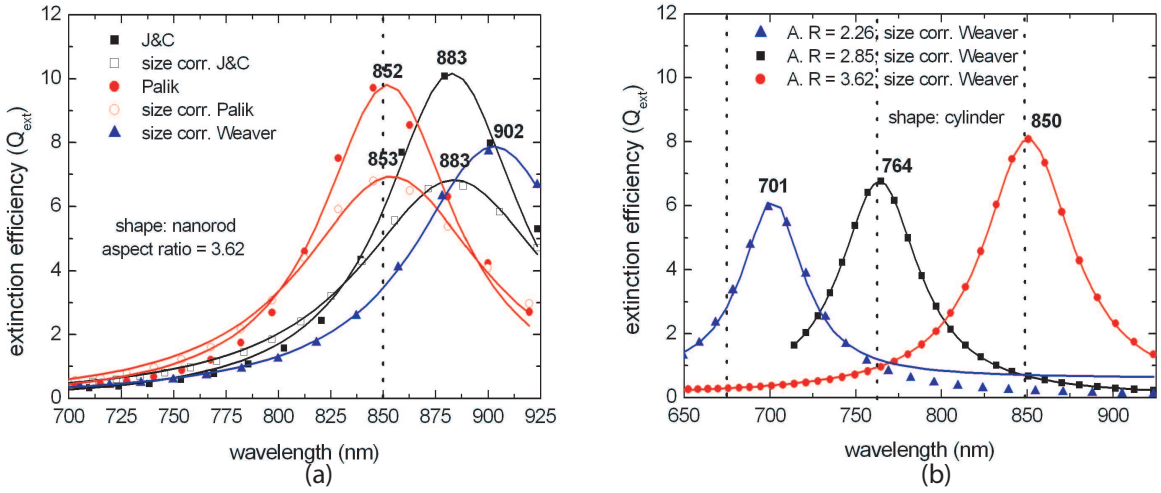

FIG. 7: (a) Simulated extinction spectrum using five different dielectric functions for particles with aspect ratio of 3.62. (b) Simulated extinction spectra of cylinders with aspect ratios of 2.26, 2.85 and 3.62 with a local refractive index of 1.33 and size corrected dielectric function from Weaver[34]. Dotted vertical lines indicate the position of experimental determined extinction maxima.

the wide spread in the position of the plasmon maximum for different sources for the dielectric function. Prior work has used one or other of these sources without justification and without recognizing the availability of other values. If one adopts the nanorod shape, it is seen that in two of the three cases, dielectric functions extracted from Palik[33] provide a good match to experiment. The dielectric function of gold from Palik[33] was determined under ultrahigh vacuum conditions which suggests reliability. Based on this and the consistency between experiment and simulation one could argue that size-corrected data from Palik[33] could be the best choice for the dielectric function. However this brings us to the case of nanorods with an aspect ratio 2.26 whose LP position does not match simulations performed with different endcap shapes and different dielectric functions where we are at a loss to explain this discrepancy.

V. CONCLUSIONS

Locating the position of the resonance maxima of GNRs using DDSCAT simulations is not trivial. This position cannot be uniquely determined and depends upon the number of dipoles used to approximate the particle, the shape used to represent the particle, and the source of dielectric function used. Further, the local environment and the sizing of the particles are important as well. The magnitude of the resonant peaks is also dependent on these factors but is less sensitive to the available choices compared with the position of peaks.

Our investigation clearly leads us to recommend the use of dipoles number higher than 30000. Examination of HR-SEM images points towards the use of hemispherically-capped cylinders for the shape of the nanorods. However it is not yet clear which dielectric function among those available is favorable to obtain best fitting between simulations and experiment though we have a good match using the data from Palik[33] in certain cases. In any case this work serves to draw attention to this drawback which has not been recognized in earlier works.

The most important conclusion that we draw from our study is that with the present approach it is not possible to objectively compare experimental data with the simulations owing to the various input parameters that can be used as tuning parameters to obtain agreement. This drawback is best exemplified in Fig. 7(b) where for a certain dielectric function source choosing a cylinder shape to represent the nanorod-contrary to structural information from electron microscopy yields a perfect match between the simulations and experiment regarding the location of the LP maximum in two cases studied.

Acknowledgements

This work is funded through the thrust area program NIMTIK of the University of Twente; through the PRESMITT project (IPD067771) of the SenterNovem program IOP Photonic Devices; and by the Nederlandse Wetenschappelijk Organisatie (NWO) and Stichting Technische Wetenschappen (STW) through project TTF 6527. The use of supercomputer facilities was made available by the Stichting Nationale Computerfaciliteiten (National Computing Facilities Foundation, NCF) with financial support from the NWO.

[1] J. Perez-Juste, I. Pastoriza-Santos, L. M. Liz-Marzan, and P. Mulvaney, Coord. Chem. Rev. **249**, 1870 (2005).

[2]P. K. Jain, I. H. El-Sayed and M. A. El-Sayed, Nano Today **2**, 18 (2007).
[3]J. W. Stone, P. N. Sisco, E. C. Goldsmith, S. C. Baxter and C. J. Murphy, Nano Lett. **7**, 116 (2007).
[4]H. Ding, K-T. Yong, I. Roy, H. E. Pudavar, W. C. Law, E. J. Bergey and P. N. Prasad, J. Phys. Chem. C. **111**, 12552 (2007).
[5]X. Huang, I. H. El-Sayed, W. Qian and M. A. El-Sayed, Nano Lett. **7**, 1591 (2007).
[6]N. Félidj, G. Laurent, J. Grand, J. Aubard, G. Lévi, A. Hohenau, F. R. Aussenegg and J.R. Krenn, Plasmonics. **1**, 35 (2006).
[7]A. L. Oldenburg, M. N. Hansen, D. A. Zweifel, A. Wei and S. A. Bopart, Opt Express. **14**, 6724 (2006).
[8]T. S. Troutman, J. K. Barton and M. Romanowski, Opt Lett. **32**, 1438 (2007.)
[9]H. Wang, T. B. Huff, D. A. Zweifel, W. He, P. S. Low, A.Wei and J-X. Cheng, Proc. Nat. Acad. Sci. **102**, 15752 (2005).
[10]N. J. Durr, T. Larson, D. K. Smith, B. A. Korgel, K. Sokolov and A. Ben-Yakar, Nano Lett. **7**, 941 (2007).
[11]C-D. Chen, S-F. Cheng, L-K. Chau and C. R. C. Wang, Biosens Bioelectron. **22**, 926, (2007).
[12]K. Kim, S. W. Huang, S. Ashkenazi, M. O'Donnell, A. Agarwal, N. A. Kotov, M. F. Denny and M. J. Kaplan, Appl Phys Lett. **90**, 223901 (2007).
[13]M. Eghtedari, A. A. Oraevsky, J. A. Copland, N. A. Kotov, A. Conjusteau and M. Motamedi, Nano Lett. **7**, 1914 (2007).
[14]C. H. Chou, Cheng. D. Chen and C.R. Chris Wang, J. Phys. Chem. B. **109**, 11135 (2005).
[15]T. B. Huff, L. Tong, Y. Zhao, M. N. Hansen, J-X. Cheng and A. Wei, Nanomed. **2**, 125 (2007).
[16]L. Tong, Y. Zhao, T. B. Huff, M. N. Hansen, A. Wei and J-X. Cheng, Adv. Mater. **19**, 3136 (2007).
[17]E. M. Purcell and C.R. Pennypacker, Astrophys J. **186**, 705 (1973).
[18]B. T. Draine and P. J. Flatau, "User Guide for the Discrete Dipole Approximation Code DDSCAT.6.1,"http://arxiv.org/abs/astro-ph/xxx.
[19]W-H. Yang, G. C. Schatz and R. R. van Duyne, J. Chem. Phys. **103**, 869 (1995).
[20]N. Félidj, J. Aubard and G. Lévi, J. Chem. Phys. **111**, 1195 (1999).
[21]A. Brioude, X. C. Jiang and M. P. Pileni, J. Phys. Chem. B. **109**, 13138 (2005).
[22]G. Yin, S-Y. Wang, M. Xu and L-Y. Chen, J. Korean. Phys. Soc. **49**, 2108 (2006).
[23]A. L. Gonzalez and C. Noguez, J. Comput. Theor. Nanosci. **4**, 231 (2007).
[24]K. S. Lee and M. A. El-Sayed, J. Phys. Chem. B. **109**, 20331 (2005).
[25]K. S. Lee and M. A. El-Sayed, J. Phys. Chem. B. **110**, 19220 (2006).
[26]P. K. Jain, K. S. Lee, I. H. El-Sayed and M. A. El-Sayed, J. Phys. Chem. B. **110**, 7238 (2006).
[27]S. W. Prescott and P. Mulvaney, J. Appl. Phys. **99**, 123504 (2006).
[28]E. S. Kooij and B. Poelsema, Phys. Chem. Chem. Phys. **8**, 3349 (2006).
[29]B. Nikoobakht and M. A. El-Sayed, Chem. Mater. **15**, 1957 (2003).
[30]R. Rayavarapu, W. Peteresen, C. Ungureanu, T. G van Leeuwen and S. Manohar, Int. J. Biomed. Imag. 29817, 29817-1 (2007).
[31]B. T. Draine and P. J. Flatau, J. Opt. Soc. Am. A. Opt. Image Sci. Vis. **11**, 1491 (1994).
[32]P. B. Johnson and R. W. Christy, Phys. Rev. B. **6**, 4370 (1972).
[33]E. D. Palik, Handbook of optical constants of solids, Academic Press, New York. 1985.
[34]J. Weaver, C. Krafka, D. Lynch and E. Koch, Physics Data: Optical Properties of Metals, Part 2: Noble Metals, Aluminium, Scandium, Yttrium, the Lanthanides and the Actinides (Fach-Informations Zentrum, Karlsruhe, 1981).
[35]C. Ungureanu, R. G. Raja, T. G van Leeuwen, S. Manohar, Proc. SPIE. **6631**, 663108 (2007).
[36]C. Pecharroman, J. Perez-Juste, G Mata-Osoro, L. M. Liz-Marzan and P. Mulvaney, Phys. Rev. B. **77**, 035418 (2008).